Global quantitative monitoring of the ion exchange balance in a chloride migration test on cementitious materials with mineral additions

Rachid Cherif, Ameur Hamami, Abdelkarim Aït-Mokhtar

Global quantitative monitoring of the ion exchange balance in a chloride migration test on cementitious materials with mineral additions

Rachid CHERIF*, Ameur El Amine HAMAMI, Abdelkarim AÏT-MOKHTAR

LaSIE UMR CNRS 7356, University of La Rochelle, Avenue Michel Crépeau, 17042 La Rochelle Cedex 1, France

*** Corresponding author:**
e-mail address: rachid.cherif@univ-lr.fr
Tel: +33 5.46.45.72.30.

Global quantitative monitoring of the ion exchange balance in a chloride migration test on cementitious materials with mineral additions

ABSTRACT

The concrete pore solution changes during chloride transfer due to the species leaching and the dissolution/precipitation of compounds. The latter could affect the material porosity and the chloride diffusion coefficient. In order to quantify these changes, the global movement of species was monitored on blended cement materials during a chloride migration test. Compartment solutions and sample pore solutions were analyzed in order to quantify the ion exchange balance. Two migration test protocols were carried out using (i) NaOH, KOH and NaCl, and (ii) synthetic seawater and synthetic pore solution. The use of slag reduces the free chloride in the porosity by about 9 times. For the Portland cement material, a precipitation of 0.3%wt of Na, 0.6%wt of K and 1%wt of Cl participated in a porosity clogging of 60%. Finally, the materials with mineral additions reduce the portlandite dissolution during chloride transfer and the calcium leaching phenomena up to 26%.

***Keywords**:* cementitious materials; mineral addition; pore solution; chlorides; dissolution/precipitation.

1. Introduction

Concrete and cement-based materials, with or without mineral additions, are porous materials that can be penetrated by external aggressive species. Among these species, we quote carbon dioxide, sulfates, de-icing or marine salts, etc. The latter present the principal risk that might affect the durability of reinforced concrete structures in marine areas. Indeed, chlorides penetrate in the cover concrete, under a concentration gradient and/or liquid pressure gradient, reach the rebar and generate their corrosion that can causes several degradations leading to a local or general ruin of the structure [1]–[3].

In the last decades, chloride transfer has been widely studied because of its important economic issues [4]–[10]. This phenomenon has been the subject of several experimental and numerical studies that were intended to propose methods and tools for predicting chloride transfer and structure service life. In fact, several methods to determine the chloride diffusion coefficient were proposed: some of them are based on the steady state migration test [11]–[13], and some consider non-steady state tests [14]–[16]. The latter allow a rapid determination of the chloride diffusivity and avoid a large part of leaching phenomena during chloride migration. Nevertheless, such methods do not consider the chemical interactions and the precipitation phenomena. Moreover, it has been shown that chloride transfer is influenced by electrochemical interactions in the layer of C-S-H (electrical double layer [17]–[20]) and by chemical interactions with the anhydrous cement (C_3A and C_4AF [21, 22]). The latter generate a formation of Friedel's and Kuzel's salts in the porosity. Furthermore, chloride diffusion or migration into the pore solution and species leaching could generate the portlandite dissolution [23]–[26]. Sutter *et al*. [25] highlighted the consumption of portlandite to form new unstable compounds such as Friedel's salt and the hydrated calcium oxychloride ($3CaO\ CaCl_2\ 15H_2O$). These phenomena affect the microstructure of

concretes, pore solution and their chloride diffusion coefficients measured by the migration test [27]–[29]. In fact, Andrade *et al*. [30], and Castellote *et al*. [31]–[34] studied the specie evolutions in the two compartments of the migration cell and the leaching of calcium and silicon accelerated by the electrical field in order to monitoring concrete degradations. Moreover, Buckley *et al.* [35] and Kyle *et al.* [36] extracted and analyzed pore solutions of a wide range of mortars and cement pastes containing sodium chloride in the mixing water. With 7.5% of chlorides by mass of cement, free chloride content of the pore solution reached a maximum of about 16%. This level is assumed to represent the saturation concentration of the solution (with pH of about 13.5). These experimental investigations did not consider: (i) all the monovalent and divalent ion exchanges of the pore solution together during the diffusion or migration of chlorides, nor (ii) the mineral additions in cementitious materials studied.

Finally, Tran *et al.* [37, 38] developed a chloride transfer model taking into account the portlandite dissolution, salt precipitation (Friedel's and Kugel's ones) and the kinetic control to predict chloride binding in concrete. The comparison between simulation results and experimental ones underlined the need to take into account, in transport modeling, the actual pore solution composition of materials and the hydrates/pore solution interactions. However, there is a lack of data in the literature on these interactions and their effects on the chemical composition of the concrete pore solution.

In this paper, we quantify the ion exchange balance during the chloride migration test. The investigations allow to study the hydrates/pore solution interactions, multispecies leaching and the composition changes of the pore solution of blended cement pastes with blast furnace slag, fly ash and silica fume submitted to the migration test (considering all ions likely to be involved in transport during the migration test). The

data will allow to better model electrochemical process and microstructure changes during transfer phenomena.

For this purpose, cement pastes were submitted to chloride migration tests. An investigation was performed on the three zones of the migration cell: the upstream compartment, the sample and the downstream compartment. On the one hand, pore solutions of materials were extracted and analyzed before and after the migration test, and on the other hand, compartments solutions were regularly analyzed. In addition, Scanning Electron Microscopy (SEM) analyses for the materials tested were performed. The investigation allows the monitoring of diffusion/leaching/precipitation phenomena and then quantifying pore solution changes resulting from these processes. Finally, an alternative protocol of the chloride migration test was used for realistically simulate the chloride transfer through the cementitious materials exposed to seawater. Data of the chloride diffusion coefficient, free chlorides in the pore solution and leaching indicators (calcium content) provided by this modified protocol of the migration test were compared to those of the usual one based on NaOH, KOH and NaCl. This comparison should indicate the appropriateness of using this modified method which should avoid too much leaching and consider more precise interactions of the pore solution ions.

2. Experimental program

2.1. Materials

Ordinary Portland cement (CEM I 52.5 N) according to the European Standard EN 197-1 was used. The mass fractions of the principal clinker phases are 65% C_3S, 13% C_2S, 7% C_3A, 13% C_4AF and 4.9% gypsum. Furthermore, blast furnace slag (BFS), fly ash (FA) and silica fume (SF) were used as a partial substitute of the cement mass. The chemical compositions of the cement and the mineral additions are given in Table 1.

Table 1

Compositions of the components used.

Composition	CaO	SiO_2	Al_2O_3	Fe_2O_3	SO_3	K_2O	Na_2O	Chlorides
CEM I (wt.%)	64.20	20.50	5.00	3.90	2.50	0.29	0.05	1.40
FA (wt.%)	5.10		85.53		0.59	2.00	1.95	0.013
BFS (wt.%)	41.50	33.30	12.50	0.40	0.50	0	0	0
SF (wt.%)	1.00	89.00	0	0	2.00	0	1.00	0.10

Four cement pastes of formulated concretes with and without mineral additions were used. These concretes were formulated using a performance-based approach similar to that used by Rozière *et al.* [39, 40] and Younsi *et al.* [41]. This approach, through the equivalent performance concept [42], is an alternative to the prescriptive approach which limits the cement replacement rate by mineral additions [43]. The performance-based approach aims at formulating a concrete with more cement substitution by mineral additions, provided that it has equivalent performance, in terms of durability, to that of the control concrete mixture. The latter complies with the prescriptive requirements for a given environment and exposure [43]. In fact, a control concrete (CC) was formulated following the Dreux-Gorisse method. Three equivalent performance concretes with mineral additions were also formulated based on the control concrete, considering a constant paste volume of all concretes (24.5% of the total volume). They are called: C_FA (30% of fly ash on the mass of binder), C_BFS (75% of blast furnace slag on the mass of binder) and C_SF (10% silica fume on the mass of binder). The calculation of the water-to-binder ratio (W/B) considers the coefficient of activity (k) of the mineral addition (binder = cement + k×addition) [43]. Since the coefficients differ between the additions used, different W/B ratios for the materials were obtained as shown in [29]: CC (W/B=0.5), C_PFA (W/B=0.40), C_PBFS (W/B=0.44) and C_PSF (W/B=0.47). Respectively, the cement pastes (CP, PFA, PBFS and PSF) relative to these formulated

concretes have been used in this study Investigations on cement pastes are easier than concretes, mainly for pore solution extraction and the representativeness of the samples.

Specimens of 11 cm diameter and 22 cm height were cast and demoulded 24 hours after manufacturing. We note that the cement paste has been mixed during the casting. Next, the surface was immediately covered with a cellophane film in order to avoid evaporation of the excess water. The manufactured cement pastes were relatively plastic after mixing given the W/B ratios. These specimens were cured during 365 days in a solution of 25 mM NaOH and 83 mM KOH [12, 44]. Afterward, samples of 6.3 cm diameter and 2.8 cm thickness for chloride migration tests were cored from these specimens.

2.2. Tests and procedures

In order to investigate the hydrates/pore solution interactions and the composition changes of the pore solution of cementitious materials during a chloride migration test, pore solutions were analyzed after their extraction from cement paste samples submitted to the migration test (during 14 days until the steady state is reached). One should recall that a rapid chloride migration test in non-steady state considerably reduces the leaching phenomena and the pore solution changes, but it does not take into account the chloride binding isotherms with cement phases and salt precipitation. In addition, analyses of compartment solutions and image processing from SEM were performed (see Fig. 1). Two migration test protocols were used: usual protocol based on NaOH, KOH and NaCl and a modified protocol using synthetic seawater at the upstream and a synthetic pore solution at the downstream. Synthetic seawater was used instead of natural seawater in order to avoid their impurities that we do not always control,

although it is more realistic. This allowed simplifying the quantitative monitoring of ion exchanges during the migration test.

The objective of this modified protocol was not to propose a new procedure to measure the diffusion coefficient. Rather, the objective was to use a laboratory test, closer to the real conditions of a structure exposed to seawater, supposed to reduce the calcium leaching from the material to the compartments. This allowed to better monitor the evolution of pore solution with chloride transport and the source of the ionic and solid/pore solution interactions as well as the Portlandite dissolution. In addition, both protocols allow comparison of the results obtained mainly for chloride diffusion coefficients and free chlorides in the pore solution.

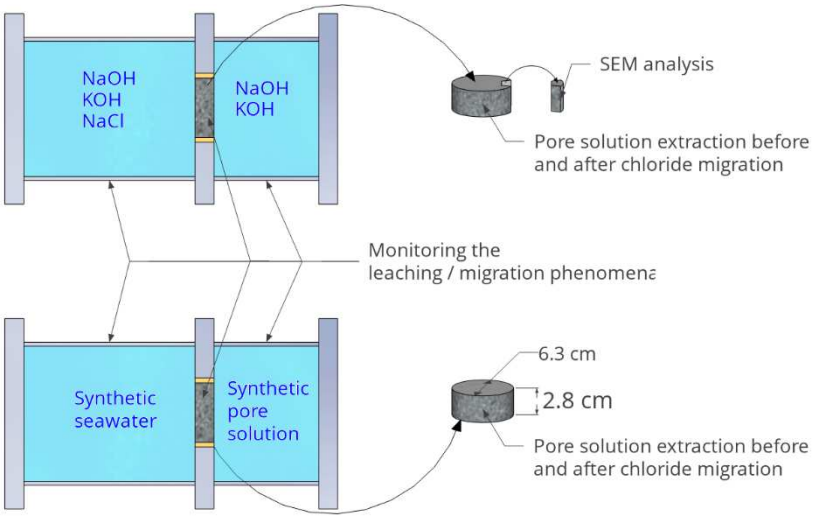

Fig. 1. Schematic representation of the two migration test protocols and material sampling for the investigation of the global ionic transport.

2.2.1. *Water and mercury porosimetry*

As suggested by the French standard NFP 18-459 [45], a vacuum saturation and a hydrostatic weighing have been used for determining the water porosity of cement pastes.

The pore size distribution of cement pastes was determined by mercury intrusion porosimetry (MIP). Measurements were performed with an Autopore III 9420 from

Micrometrics® whose pressure range reaches more than 400 MPa and covers pore diameters from 0.003 to 360 µm. Finally, the diameter is calculated from the applied pressure following Washburn-Laplace laws considering the pores as cylindrical. The technique is widely used in literature and remains the most optimal for measuring pore sizes distribution [46]–[49].

2.2.2. *Migration test*

The migration cell firstly used by Andrade [11] and developed by Aït-Mokhtar *et al.*[50] was used to determine the effective chloride diffusion coefficient at the steady state. The cell contains two compartments (upstream and downstream) separated by the test sample. Two electrodes were placed on both extremities of the cell and two reference electrodes on both sides of the sample for applying a constant electrical field of 300 V. m^{-1}. For this study, two protocols of migration test were used. The first one was based on basic solution in the compartments (composed of 25 mM of NaOH and 83 mM of KOH [12, 51]). Afterwards, the upstream solution is replaced by a solution containing 500 mM of NaCl. The second protocol was based on synthetic seawater in the upstream and the synthetic pore solution of the tested material in the downstream. We note that the compartment solutions were renewed every day during the test (14 days) to maintain constant conditions in both sides of the specimens.

2.2.3. Pore solution extraction

In order to extract the pore solution from cement pastes, a device from Cad Instruments® was used as per the method described by Longuet *et al.* [52] and developed by Barneybek and Diamond [53]. A piston is inserted above a cylindrical chamber containing the cement paste sample of about 137 cm^3 (cylinder of 5 cm diameter and 7 cm height). The sample was compressed by means of a hydraulic press. For a better efficiency, several cycles with two loading steps were applied: a loading of

0.02 MPa·s^{-1} during 15 min followed by an idle phase for 5 min. This technique presented a yield of about 17% to 22% with an applied load until 140 MPa [54]. Finally, 8 ml in average of pore solution was collected. The amount remains representative of that of the bulk of the pore solution [53].

Chemical analyses of the pore solution extracted before and after the migration test were performed with an 883 Basic Ion Chromatograph Plus from Metrohm® whose accuracy is 10^{-3} mg. l^{-1}.

2.2.4. Environmental scanning electron microscopy analyses (ESEM)

Scanning electron microscopy images and elemental analysis spectra were obtained with a scanning electron microscope (Quanta 200 FEG/ESEM) coupled with an EDAX Genesis EDS system for X-ray microanalysis. The observations were performed in environmental mode. This technique does not require preparations for the surface of cement pastes tested which avoids any possible microstructure disturbing [55, 56]. The observations were performed under a low pressure (1.5 mbar) and an acceleration voltage range between 15 and 20 kV.

3. Results and discussion

3.1. Intrinsic properties

Results of the total porosity and its standard deviation from three measurements of cement pastes are shown in Table 2. The porosity of CP is higher than ones of PFA, PBFS and PSF. This is due to the high W/B ratios of CP compared to ones of the other cement pastes used (see Section 2.1). In addition, pore size distributions and critical diameters, measured by MIP, of cement pastes used are illustrated in Fig. 2. Results show that pore size distributions are globally monomodal with a critical pore diameter of 70, 45, 8 and 70 nm for CP, PFA, PBFS and PSF, respectively. We note that the use of 10% silica fume

should have refined the porosity and the critical pore diameter of the cementitious material [57]–[59]. However, Fig. 2 shows that the critical diameters of CP, PFA and PSF were relatively similar. The difference is explained by the mixing of the cement paste PSF without superplasticizer, which could generate a non-optimized microstructure given its high water demand. Finally, PBFS has a low critical pore diameter, which is in accordance with literature showing that the blast furnace slag refines the microstructure [60].

Table 2

Water porosity and effective chloride diffusion coefficient of the cement pastes using the standard (usual) migration test.

Materials	CP	PFA	PBFS	PSF
Water porosity (%)	34.2 ± 0.2	28.5 ± 0.3	29.4 ± 0.5	29.9 ± 1.3
D_{eff} (x10^{-12} m^2/s)	5.64 ± 0.78	4.75 ± 0.63	2.38 ± 0.47	5.96 ± 1.13

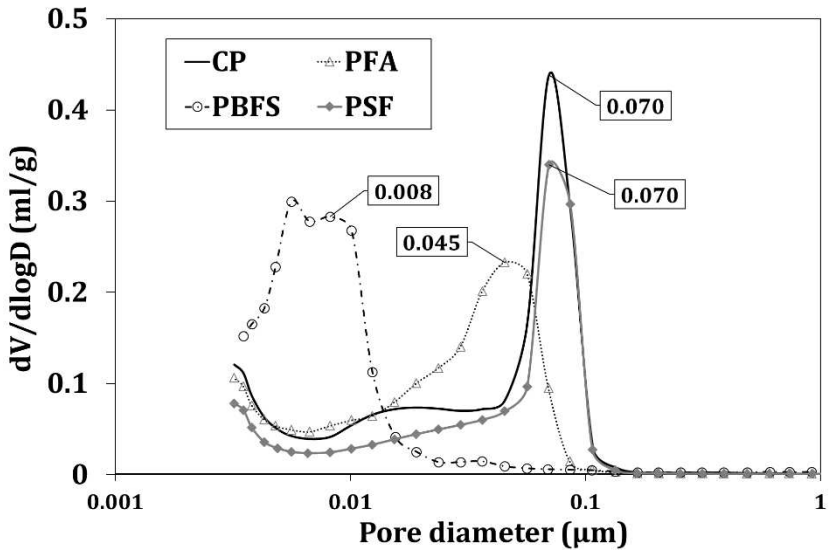

Fig. 2. Pore size distributions of the materials before the migration test.

Table 2 shows the chloride diffusion coefficient and its standard deviation from three measurements of the tested cement pastes. Firstly, chloride diffusion coefficients of CP, PFA and PSF are of the same order of magnitude, although silica fume should have reduced it [61]. This is due to the non-optimized PSF microstructure as mentioned

above. The chloride diffusion coefficient of PBFS is lower than that of CP, PFA and PSF. This is due to the replacement of cement by 75% of blast furnace slag that refines the porosity, as shown in Fig. 2, and increases the material's capacity for the chloride electrochemical fixation (physical interaction of chlorides with pore walls). This phenomenon decreases the chloride diffusion coefficient [5, 6].

3.2. Evolution of the pore solution according to the type of the conducted migration test

3.2.1. Migration test based on NaOH, KOH and NaCl

For this method, cement pastes CP, PFA, PBFS and PSF after 365 days of curing were used. Pore solution results, before and after the migration test, with standard deviations from three measurements are presented in Figs. 3 to 6. Hydroxyl concentrations were calculated by Eq. (1) based on the electroneutrality of the solution. In the following sections, the initial compositions of the pore solution before the migration test are firstly discussed. Then, the composition evolutions will be given for alkalis, chlorides, calcium, sulfates and magnesium, respectively.

$$\sum z_i C_i = 0 \tag{1}$$

where i refers to the ion analyzed (Na^+, K^+, Ca^{2+}, SO_4^{2-}, Mg^{2+} and OH^-), z is its valence, and C is its concentration.

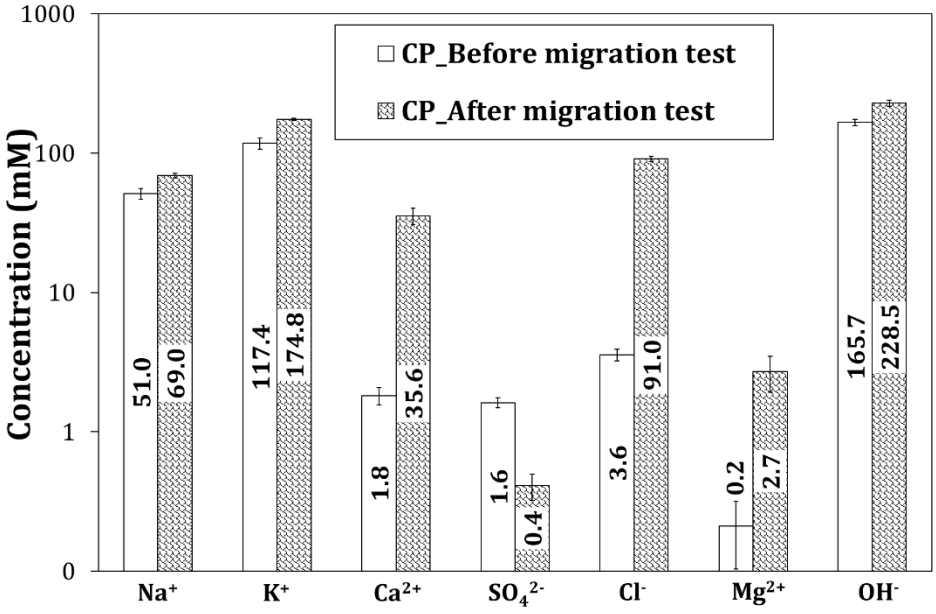

Fig. 3. Chemical composition of CP pore solution before and after the migration test.

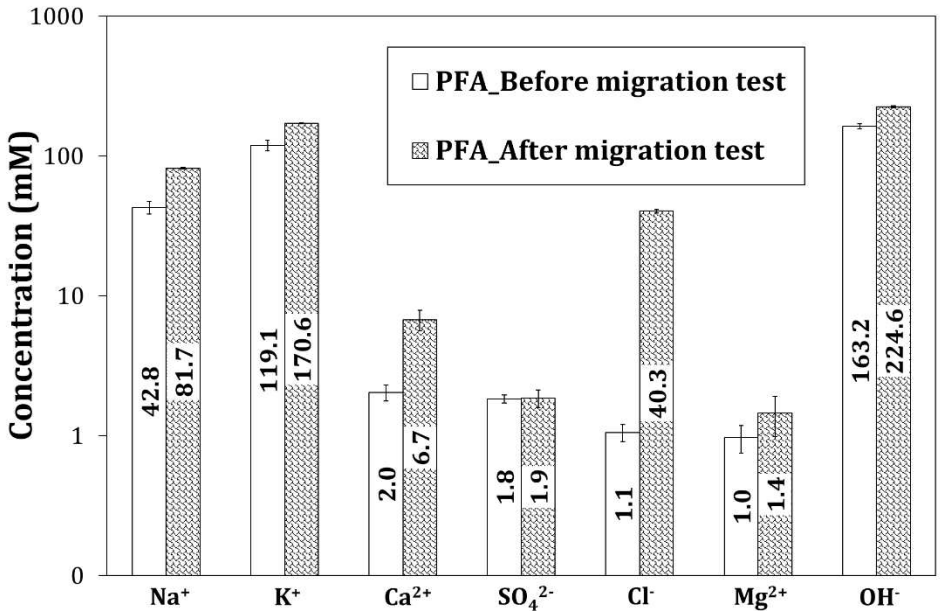

Fig. 4. Chemical composition of FA30 pore solution before and after the migration test.

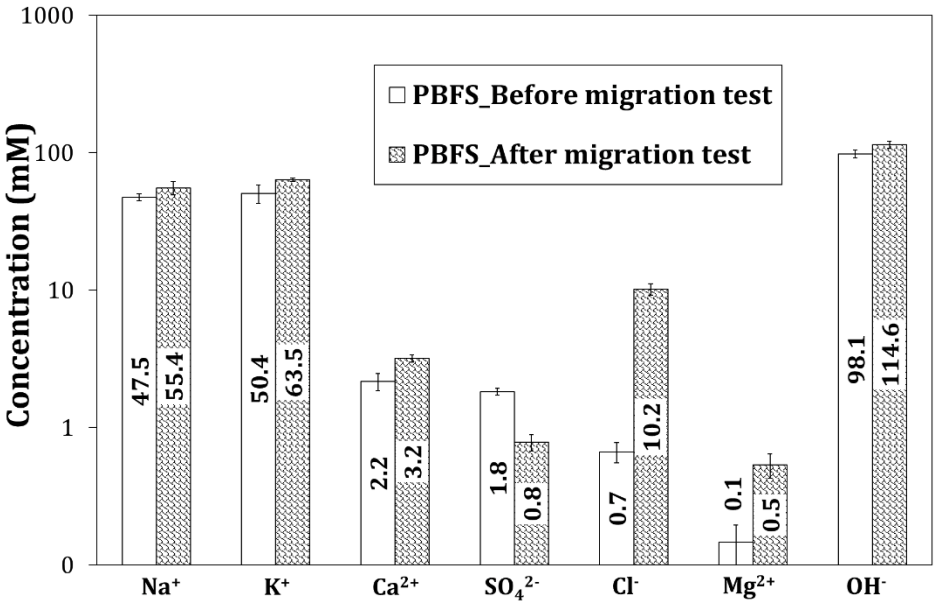

Fig. 5. Chemical composition of PBFS pore solution before and after the migration test.

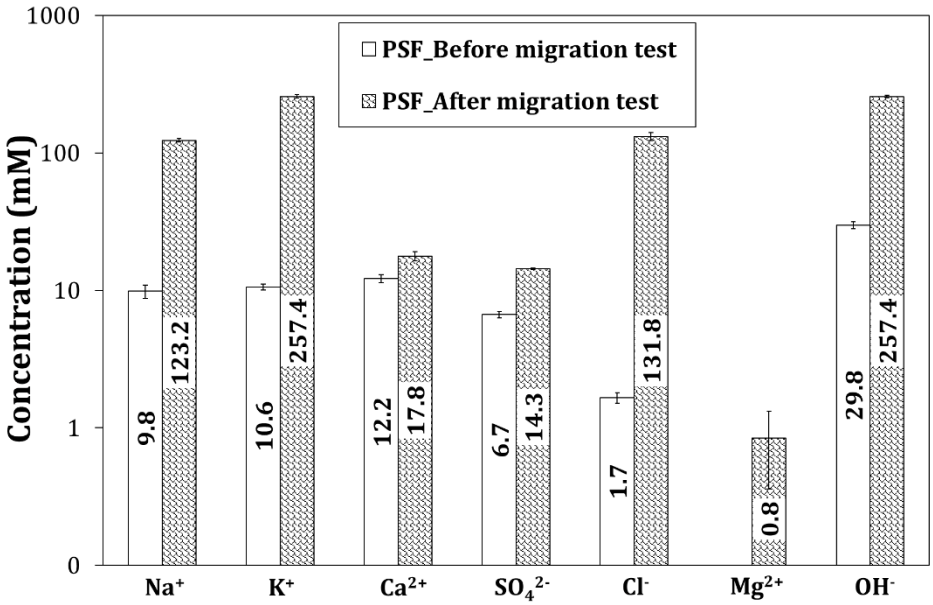

Fig. 6. Chemical composition of PSF pore solution before and after the migration test.

Firstly, we confirm that pore solutions of CP, PFA and PBFS before the migration test are mainly composed of sodium and potassium, which is in accordance with the literature [62]. Furthermore, the use of 75% of slag (PBFS), which is poor in potassium (see Table 1), decreases the concentration of this ion in the pore solution by about 2.2 times compared to CP and PFA. Note that the concentrations of divalent ions (calcium and sulfates) of CP, PFA, PBFS and PSF are relatively significant. Moreover, the replacement of Portland cement by 10% of silica fume (PSF) significantly changes the pore solution

composition. It decreases the sodium and potassium concentrations by about 5 and 11 times, respectively, compared to CP. This is due, on the one hand, to the silica fume composition based on silica instead of alkalis, and on the other hand, to the pozzolanic reaction of silica fume. The reaction leads to the adsorption of alkalis on silica surfaces [63, 64]. However, calcium and sulfate concentration of PSF are high (6 and 3 times, respectively, higher than that of CP). The divalent ion concentrations are in agreement with the literature [62, 65] Indeed, Andersson *et al*. [62] showed that the calcium amount of the cement paste with silica fume is higher than ones with blast furnace slag or fly ash, although calcium is consumed by silica to form C-S-H during the pozzolanic reaction of silica fume [63, 64]. Moreover, the high sulfate amount of PSF is due to the chemical composition of the sulfate-rich silica fume (see Table 1). In addition, Lobo and Cohen [65] showed a reduction of the ettringite formation and sulfate consumption after 48 hours of hydration of cement paste with silica fume, although the amounts of anhydrous cement and sulfates in the pore solution were still significant.

Chemical analyses of material pore solution submitted to the migration test (14 days) showed an increase of the concentration of monovalent and divalent species compared to the initial ones before the migration test. Indeed, alkalis increase for CP, PFA and PBFS ranging between 1.2 to 1.9 times for sodium and 1.3 to 1.5 for potassium. The increase is due to their diffusion or possible attraction by anion migration from the upstream to the material, mainly hydroxyls and/or chlorides [11, 29]. Concerning PSF, initially poor in alkalis, the increase in sodium and potassium concentrations was of about 13 and 24 times, respectively. The high increase is due to: (i) the alkali attraction by anions from the upstream to the material, and (ii) the possible release of these alkalis, initially chemisorbed in silica surfaces of the PSF. Moreover, chemical results highlighted the presence of free chlorides in the pore solution. We noted that the PBFS had the

lowest free chlorides compared to the rest of cement pastes tested. This is in agreement with the PBFS capacity for the chloride electrochemical fixation [5, 6].

In addition, the increase of Ca-concentration, mainly for CP (19.8 times), is due to the portlandite dissolution during chloride migration [23]–[26], as some of the portlandite participates in the formation of Friedel's salts and oxychlorides. The latter are responsible for maintaining the thermodynamic equilibrium hydrates/pore solution during chloride migration [25]. Dealing with sulfates, the evolution of their concentration presents different variations for the materials used. It depends on the sulfates released by C-S-H, their migration to the downstream under the electrical field, and the possible formation of monosulfoaluminates and trisulfoaluminates [66]. Finally, the magnesium concentration in cementitious materials remains relatively very low (it ranges between 0.5 and 3 mM).

In order to confirm these interpretations, solutions of the upstream and downstream compartments of the migration cell were also dosed to determine ion concentrations that diffused from the material to the cell compartments and vice versa. The obtained data allow better explaining the pore solution evolution during chloride transfer necessary for chloride modeling. Figs. 7 and 8 show the concentration of species diffused (leached) from the material to the upstream and the downstream, respectively. This diffusion expresses a concentration gain in the compartment with positive values (difference between the final concentration at the end of the migration test and the initial concentration of the correspondent species). Similarly, the concentration of species diffused from the compartment to the material were determined (loss with negative values).

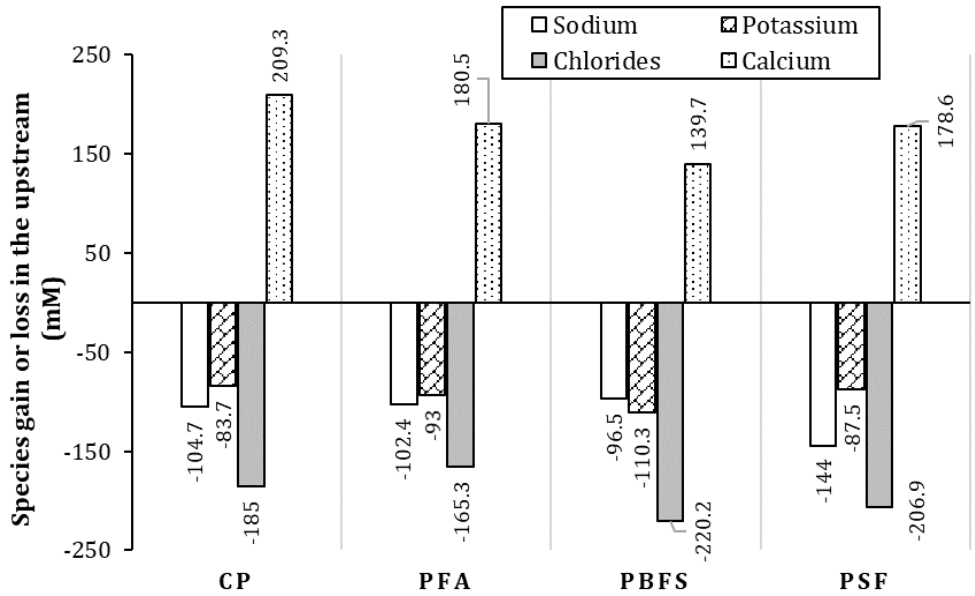

Fig. 7. Ion concentration gain or loss at the upstream at the end of the migration test.

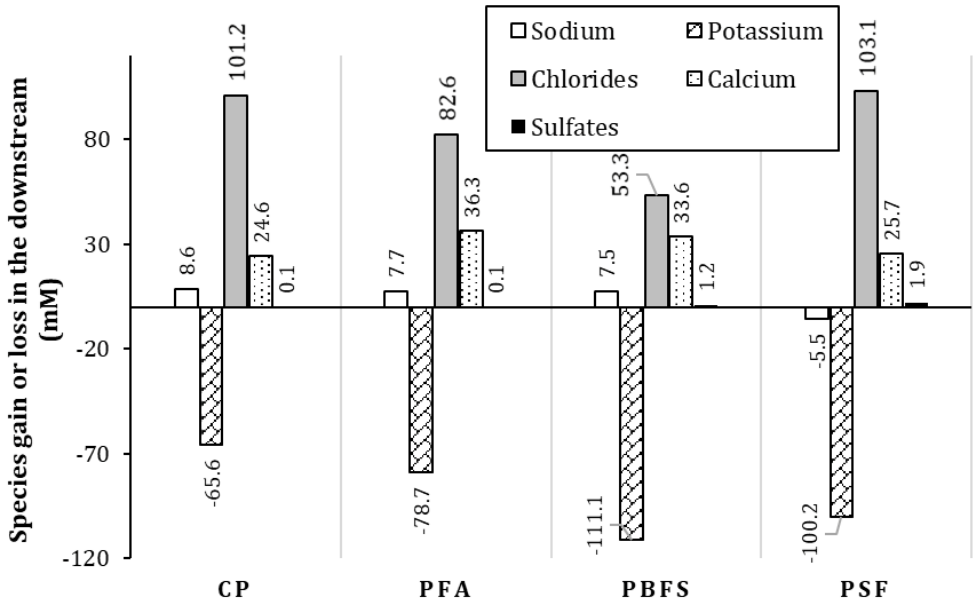

Fig. 8. Ion concentration gain or loss at the downstream at the end of the migration test.

For the upstream, chemical analyses show a loss of alkalis (potassium and sodium), that could be diffused or attracted by anions (hydroxyls and chlorides) during their migration to the material [11, 29]. The same remark could be done for the downstream compartment with a loss of potassium due to its migration from the downstream to the material under an electrical field. However, the sodium concentration at the downstream remains relatively constant. The latter could be explained by a possible balance between the sodium attracted by anions and the sodium diffusing from the

downstream to the material under the electrical field [11, 29]. Note that the balance depends on the electric field strength applied during the migration test.

An important concentration of calcium was noted in the upstream compartment (more than 140 mM). The concentration is higher than the initial one present in the pore solution before the migration test for all cement pastes tested (1.8 to 12.2 mM, see Figs. 3 to 6). The calcium diffuses from the material to the upstream under: (i) a concentration gradient between the pore solution and the upstream, and (ii) the electrical field, mainly following the portlandite dissolution during the migration test [23]–[26]. However, the calcium in the downstream compartment was relatively low compared to the upstream (less than 36 mM for all the materials). Furthermore, sulfate concentrations in compartments were very low and negligible (less than 2 mM for all the materials). Finally, the total chloride content in the material can be deduced from the difference between the chlorides lost in the upstream and those diffused to the downstream (chlorides gain in the downstream). Details are given in Table 3.

The results of the ion concentrations diffused/leached in the three zones of the migration test (upstream, downstream and the sample tested) could be used to calculate the transference numbers of all the considered species. These transference numbers define the amount of current transported by each species in the solution during the migration test [11, 31]. They are key parameters in the multispecies modeling of chloride transport in the cementitious materials.

Table 3 synthesizes the results obtained from the analyses of the three zones of the migration cell using NaOH, KOH and NaCl. The synthesis allows: (i) quantifying the species precipitated in the porosity during chloride transfer, mainly the concentration of sodium, potassium and chlorides; (ii) validating the accuracy and consistency of

monitoring of the leaching and diffusion phenomena in the migration cell (closed system). Thereafter, we study the calcium released from the portlandite dissolution.

The values in Table 3 represent the ion concentration gain (positive values) or loss (negative values) during the 14 days of the migration test: (i) of the two compartments (table rows: “upstream” or “downstream”), and (ii) of the material pore solution (table rows: “pore solution”). The latter are the difference between the ion concentration in the pore solution before and after the migration test. Finally, we present the ion concentrations which participated in the salt precipitations in the porosity and the microstructure changes (table rows: “Precipitated in the sample”). They are deduced from the ion concentration gain or loss of the compartments and the pore solution (ion precipitated = ion diffused to the material − ion gain in the pore solution). We note that the ion concentration gain of the pore solution represents the amount of the diffused ion in the pore solution volume at the end of the test (pore volume for saturated material).

Table 3

Ion concentration gain or loss for the pore solution and compartments and ions precipitated in the material at the end of the migration test.

Materials	Zone	Sodium (mM)	Potassium (mM)	Chlorides (mM)	Calcium (mM)	Sulfates (mM)
CP	Upstream	– 104.7	– 83.7	– 185.0	209.3	0
	Pore solution	18	57.4	87.4	33.8	– 1.2
	Downstream	8.6	– 65.6	101.2	24.6	0.1
	Precipitated in the sample	95.6	147.6	81.2	-	-
PFA	Upstream	– 102.4	– 93	– 165.3	180.5	0
	Pore solution	38.9	51.5	39.2	4.7	0.1
	Downstream	7.7	– 78.7	82.6	36.3	0.1
	Precipitated in the sample	93.7	170.4	81.7	-	-
PBFS	Upstream	– 96.5	– 110.3	– 220.2	139.7	0
	Pore solution	7.9	13.1	9.5	1	– 1
	Downstream	7.5	– 111.1	53.3	33.6	1.2
	Precipitated	88	221.1	166.6	-	-
PSF	Upstream	– 144	– 87.5	-206.9	178.6	0
	Pore solution	113.4	246.8	130.1	5.6	7.6
	Downstream	– 5.5	– 100.2	103.1	25.7	1.9
	Precipitated in the sample	146.5	181.3	100.4	-	-

The results of the alkalis and chlorides precipitated in the sample and the calcium released could be used to estimate the clogged/created porosity during chloride transfer. Firstly, precipitate phases are confirmed by a comparison of SEM images coupled to the energy dispersive X-ray microanalysis (EDX). This technique allowed for measuring the elemental distribution of the precipitated compounds, at the microscopic level, for CP, PFA and PBFS, before and after the migration test (see Figs. 9 to 11). In fact, elemental distributions confirm the precipitation of alkalis (up to 1%wt for sodium and 1.6%wt for potassium for PFA) and chlorides (up to 1.7%) in the materials after 14 days

of migration test. Monitoring the precipitated calcium remains relatively difficult. It requires the distinction between the calcium released by the portlandite dissolution and the one participating in the precipitation of salts, e.g. portlandite is consumed by the formation of calcium oxychloride [25]. For this purpose, further experimental investigations are required.

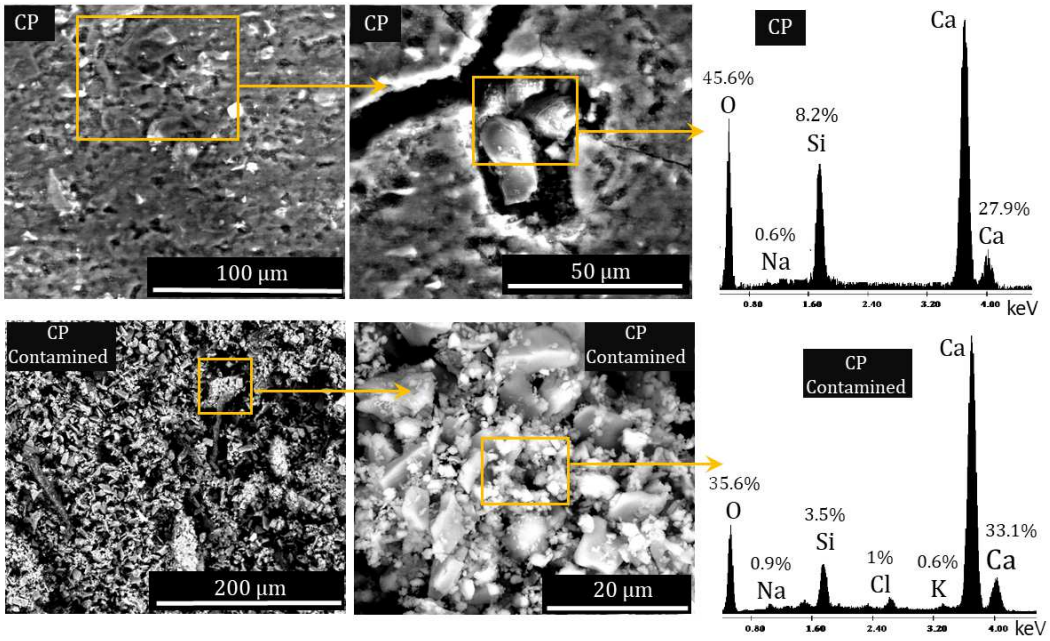

Fig. 9. SEM images and EDX spectra of CP with and without chloride contamination.

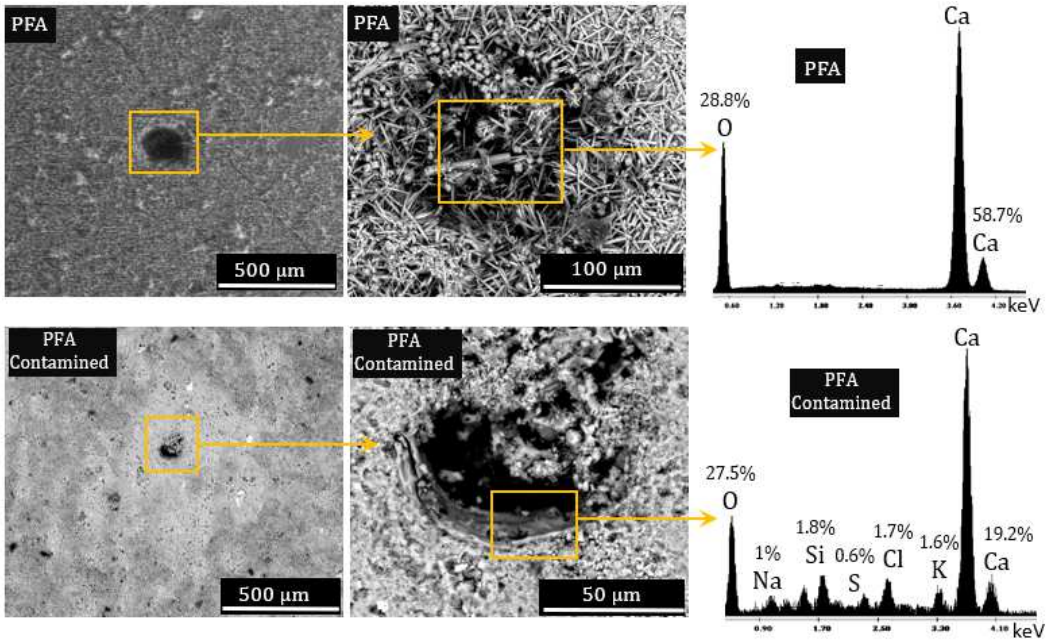

Fig. 10. SEM images and EDX spectra of PFA with and without chloride contamination.

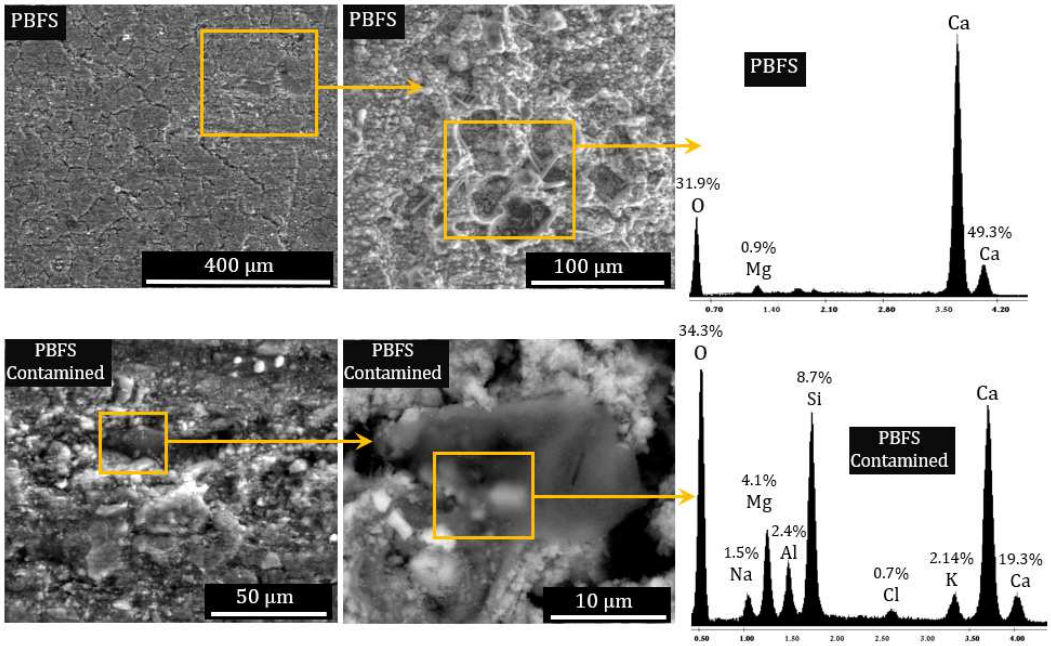

Fig. 11. SEM images and EDX spectra of PBFS with and without chloride contamination.

The changes in porosity during the migration test were calculated from the volume of precipitated/dissolved phases as follows:

- Calculation of the volume of clogged porosity (V_{clog} with negative values) from the concentration (C [M]) of alkalis and chlorides precipitated shown in Table 3 (using

the density (ρ [g/cm^3]), the molar mass (M [g/mol]) of each species and the volume of the solution where concentrations were measured, see Eq. (2));

$$V_{clog} = \frac{C \times M \times V_{upstream}}{\rho} \quad (2)$$

- Calculation of the volume of the created porosity (V_{creat} with positive values) from the concentration of the calcium released by the portlandite dissolution, see Eq. (3);

$$V_{creat} = \frac{C \times M \times V_{upstream}}{\rho} \quad (3)$$

- Deduction of the rate of the porosity changes, $\Delta\phi$, as follows:

$$\Delta\phi = \frac{V_{clog} + V_{creat}}{V_{voids}} \quad (4)$$

Table 4 shows the porosity volume changes of the tested materials. The chloride migration generates a porosity reduction of about 23% for CP and 40 to 58% for cement pastes with mineral additions, without considering the possible precipitation of aluminum and sulfates, which can further reduce the porosity. Portlandite-rich CP increases its dissolution and then slows down the porosity reduction, compared to PFA and PSF [29]. In general, calculations of the porosity change are in agreement with the experimental investigations presented in a previous work [29]. The latter show further details about the effect of chloride migration on the pore size distribution and critical diameter of the material.

Table 4

Porosity changes due the precipitation/dissolution phenomena during the chloride migration test.

Materials	Phenomenon	Species participated	Volumes clogged (-) created (+) (cm^3)	Porosity changes (%)
CP (V_{voids}=30 cm^3)	Compounds precipitation	V_{clog} (Na)	−4	−23
		V_{clog} (K)	−12	
		V_{clog} (Cl)	−3	
	Portlandite dissolution	V_{creat} (Ca)	+12	
PFA (V_{voids}=25 cm^3)	Compounds precipitation	V_{clog} (Na)	−4	−40
		V_{clog} (K)	−13	
		V_{clog} (Cl)	−3	
	Portlandite dissolution	V_{creat} (Ca)	+10	
PSF (V_{voids}=26 cm^3)	Compounds precipitation	V_{clog} (Na)	−6	−58
		V_{clog} (K)	−15	
		V_{clog} (Cl)	−4	
	Portlandite dissolution	V_{creat} (Ca)	+10	

Due to the porosity and the pore size distribution of PBFS, the precipitation of new salts does not simply occur in its small pores (see Fig. 2) [67]. Therefore, the estimation of the porosity changes of PBFS requires further investigations of its microstructure and the process of salt precipitation such as X-ray microtomography and/or X-ray diffraction analyses (XRD).

3.2.2. Migration test based on synthetic seawater and synthetic pore solution

In order to reduce the calcium leaching noted for the standard migration test, a modified migration test protocol was performed during 14 days using a synthetic seawater in the upstream compartment, similar to the seawater of the French Atlantic coast (see Table 5) and synthetic pore solution of the tested material at the downstream. This

laboratory protocol of the migration test, closer to the real conditions of multispecies transfer in reinforced concrete structures, allowed to better monitor: (i) the pore solution evolution, mainly the Ca-concentration increase in the material during chloride migration; and (ii) the portlandite dissolution, which we could not correctly control with the standard migration test based on NaOH, KOH and NaCl. Synthetic solutions have been prepared by dissolving hydrated chemical products in distilled water in order to reproduce exactly the natural solution. We note that the migration cell compartments have been cleaned regularly with distilled water before each solution renewal in order to avoid any possible ionic contaminations.

Table 5

Chemical composition of the synthetic seawater used [68, 69].

	Na^+	K^+	Ca^{2+}	SO_4^{2-}	Mg^{2+}	Cl^-	OH^-
Ionic concentration of synthetic seawater (mM)	485	10	10	29	55	565	2

For this method, the same pastes as previously mixed with distilled water were used. In order to differentiate the materials tested for this second protocol from the first one (protocol with NaOH, KOH and NaCl), a star was added to their names (CP*, PFA*, PBFS* and PSF*), meaning that materials were mixed with distilled water instead of tap water. Pore solution of materials was extracted and analyzed before and after the migration test. Results are presented in Figs. 12 to 15. One should note that the synthetic solution used in the downstream compartment is the same as the one extracted from the materials before the migration test.

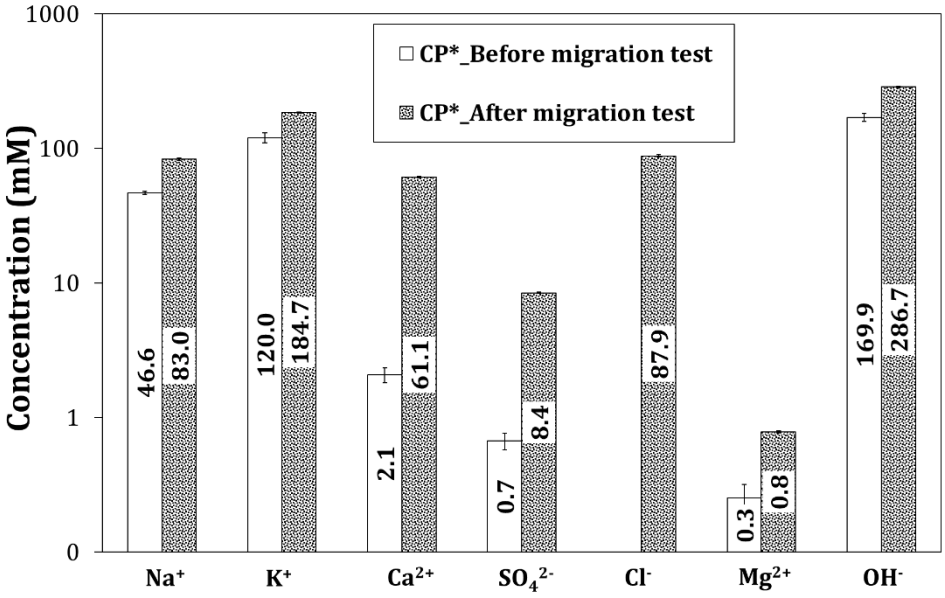

Fig. 12. Chemical composition of CP* pore solution before and after the migration test.

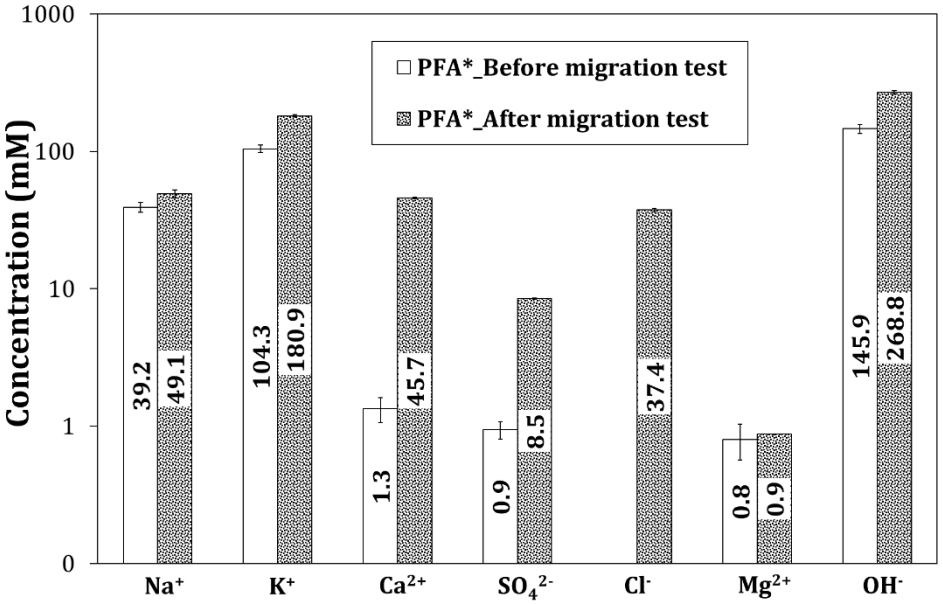

Fig. 13. Chemical composition of FA30* pore solution before and after the migration test.

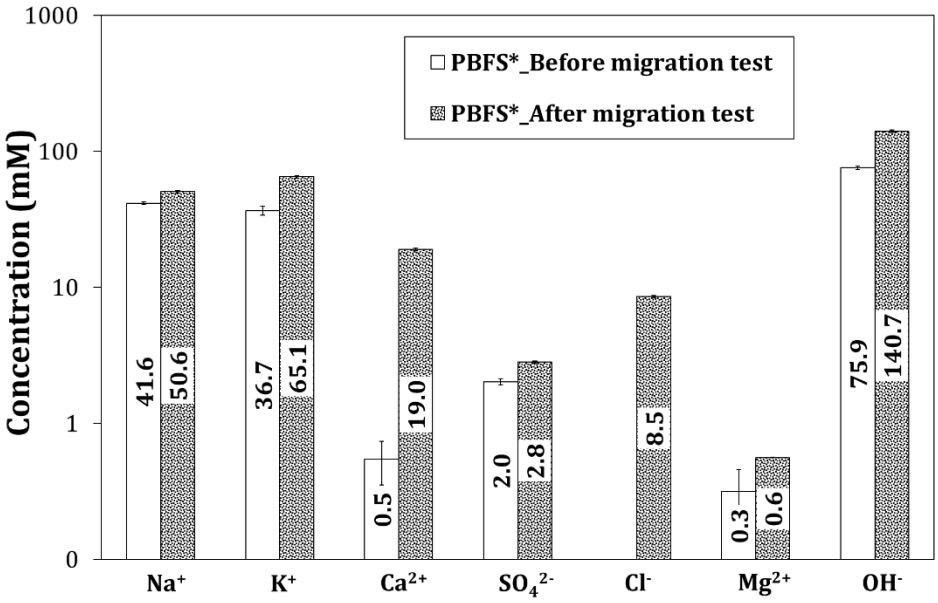

Fig. 14. Chemical composition of PBFS* pore solution before and after the migration test.

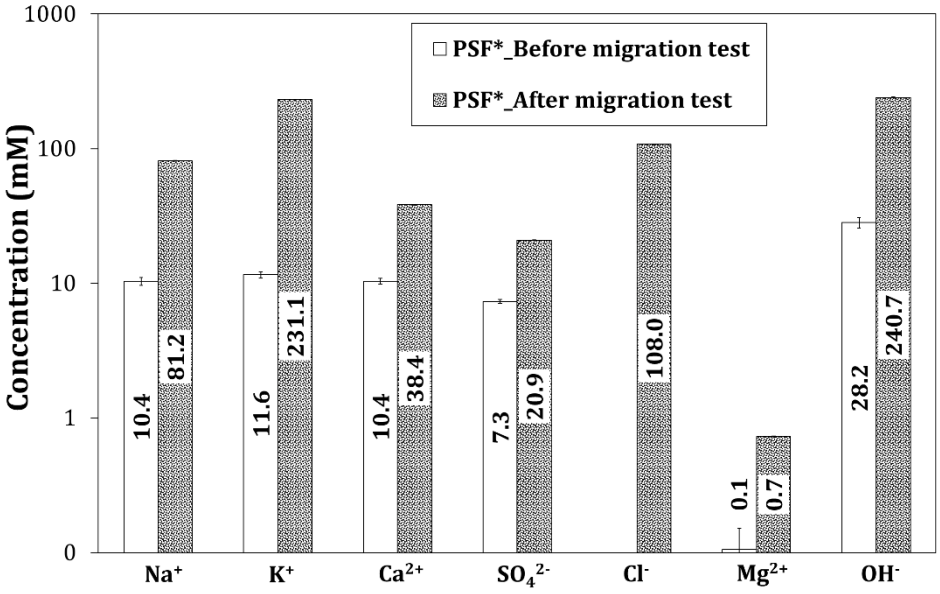

Fig. 15. Chemical composition of PSF* pore solution before and after the migration test.

Firstly, chemical compositions of healthy materials (not exposed to chlorides) are in agreement with those of materials mixed with tap water (Figs. 3 to 6). However, the chloride concentration for cement pastes made with distilled water was lower, even negligible.

Although seawater is poor in potassium (10.6 mM), evolutions of pore solution for this second protocol of migration test are in agreement with the first one. For the three

materials CP*, PFA* and PBFS*, the increase of sodium and potassium concentrations ranges between 1.2 to 1.8 times and 1.5 to 1.8 times, respectively. PSF* pore solution showed an increase of alkalis of about 8 times of sodium and 20 times of potassium that is due to: (i) their diffusion or attraction by anion migration from the upstream to the material, and (ii) their releasing by silica surface, as shown above [29, 64]. Moreover, results of free chlorides diffused to the pore solution for both methods are in accordance. A low concentration of free chlorides for PBFS* was noticed because of the replacement of cement by 75% of blast furnace slag that increase the material's capacity for the chloride fixation [60]. Finally, chemical analyses of the pore solutions show a Ca-increase during chloride migration, which is higher than that observed in the standard migration test (see Section 3.2.1). This is due to the presence of calcium in the compartment solutions used (synthetic seawater and synthetic pore solution), which reduces its concentration gradient with the material and then reduces its leaching in the upstream. The Ca-leaching process could affect the chloride diffusivity and the material microstructure submitted to a migration test, in particular at the anodic side (in contact with the downstream compartment) [28, 70]. That is why comparisons of the diffusion coefficients and the free chlorides of the materials subjected to both protocols of migration tests were performed. Results, shown in Table 6, highlight that the use of the synthetic seawater and synthetic pore solution reduces concentration gradients between the material tested and the cell compartments but do not affect the chloride diffusion coefficient and the concentration of free chlorides in the pore solutions, compared to the standard migration test based on NaOH, KOH and NaCl. In fact, as for the usual protocol, during the modified migration test, the portlandite dissolves either because of the electric field [71] or to re-balance the thermodynamic system with the consumption of calcium to form Friedel's salt and hydrated calcium oxychloride [23]–

[26]. The portlandite dissolution and the release of the alkalis chemisorbed in silica (for PSF [64]) again creates a concentration gradient between the material and the upstream compartment and causes species leaching. Certainly, the latter remains relatively low compared to the standard protocol of the migration test, but it does not necessarily affect the chloride diffusion coefficient measured.

Table 6

Comparison between chloride diffusion coefficients and free chlorides for materials subjected to the two types of migration tests (usual and modified protocol).

	CP	PFA	PBFS	PSF
D_{cl}_usual protocol (x10^{-12} m^2/s)	5.64	4.75	2.38	5.96
D_{cl}_modified protocol (x10^{-12} m^2/s)	5.02	5.36	1.92	5.27
Free chlorides_usual protocol (mM)	87.4	39.2	9.5	130.1
Free chlorides_modified protocol (mM)	87.9	37.4	8.5	108.0

4. Conclusion

The aim of this work was to perform a global assessment of ion transport in a chloride migration test carried out on blended cement materials. The materials contain blast furnace slag, fly ash and silica fume. From the obtained results, following main conclusions are made:

- The use of 75% of slag increases the material's capacity for the chloride fixation in C-S-H and consequently reduces the free chloride concentration in the pore solution by 9 times compared to the Portland cement pastes.
- For the cement pastes with 30% of fly ash submitted to a migration test, up to 1%wt of sodium and 1.6%wt of potassium precipitate in the material porosity.
- Despite the use of silica fume or fly ash that consume the portlandite to form C-S-H due to pozzolanic reaction, about 40% of porosity increase (10 cm^3 of volume

created) was noticed at the end of the migration test due to the dissolution of the portlandite.

- Because of the precipitation of alkalis and chlorides accompanied by the dissolution of the portlandite, a porosity clogging of 23% of CP, 40% of PFA and 58% of PSF was estimated, without considering the precipitation of calcium, aluminum and sulfates that could further reduce the porosity.
- At the end of the migration test, the alkali content of the pore solution of the materials increases by about 1.2 to 1.9 times for sodium and 1.3 to 1.5 for potassium. These species are diffused or attracted by anions to the material. In addition, a significant pore solution change was noticed for cement paste with silica fume (8 times that of sodium and 20 times that of potassium). These species, initially chemisorbed in silica surfaces, were released during the migration test.
- The use of a synthetic pore solution and synthetic seawater for the migration test slightly reduced the calcium leaching in the upstream because of the portlandite dissolution that disturbs the Ca-equilibrium in the migration cell. Moreover, comparison between chloride diffusion coefficients obtained by both migration test protocols used does not justify the need to modify the standard test procedure, considering also: (i) the need for extraction test for the synthetic pore solution; and (ii) that the composition of seawaters differs from one place to another.

Declarations of interest: none

Funding sources

This research did not receive any specific grant from funding agencies in the public, commercial, or not-for-profit sectors.

Acknowledgments

The authors would like to thank Dr. E. Conforto for the realization of SEM images and the NEEDS program for having supported this work.

5. References

[1] O. Poupard, A. Aït-Mokhtar, P. Dumargue, Impedance spectroscopy in reinforced concrete: Procedure for monitoring steel corrosion. Part I: development of the experimental device, J. Mater. Sci. 38 (2003) 2845–2850.

[2] O. Poupard, A. Aït-Mokhtar, P. Dumargue, Impedance spectroscopy in reinforced concrete: Experimental procedure for monitoring steel corrosion: Part II: polarization effect, J. Mater. Sci. 38 (2003) 3521–3526.

[3] C. Andrade, Propagation of reinforcement corrosion: principles, testing and modelling, Mater. Struct. 52 (2019) 1-26.

[4] O. Amiri, A. Aït-Mokhtar, A. Seigneurin, A complement to the discussion of A. Xu and S. Chandra about the paper «Calculation of chloride coefficient diffusion in concrete from ionic migration measurements» by C. Andrade, Cem. Concr. Res. 27 (1997) 951–957.

[5] O. Amiri, A. Aït-Mokhtar, P. Dumargue, G. Touchard, Electrochemical modelling of chloride migration in cement-based materials. Part I. Theoretical basis at microscopic scale, Electrochim Acta 46 (2001) 1267–1275.

[6] O. Amiri, A. Aït-Mokhtar, P. Dumargue, G. Touchard, Electrochemical modelling of chlorides migration in cement-based materials. Part II. Experimental study—calculation of chlorides flux, Electrochim. Acta 46 (2001) 3589–3597.

[7] C. Andrade, M. Prieto, P. Tanner, F. Tavares, R. d'Andrea, Testing and modelling chloride penetration into concrete, Constr. Build. Mater. 39 (2013) 9–18.

[8] M. Otieno, H. Beushausen, M. Alexander, Effect of chemical composition of slag on chloride penetration resistance of concrete, Cem. Concr. Compos. 46 (2014) 56–64.

[9] Y. Tissier, V. Bouteiller, E. Marie-Victoire, S. Joiret, T. Chaussadent, Y. Tong, Electrochemical chloride extraction to repair combined carbonated and chloride contaminated reinforced concrete, Electrochimica Acta 317 (2019) 486–493.

[10] T. Sanchez, P. Henocq, O. Millet, A. Aït-Mokhtar, Coupling PhreeqC with electro-diffusion tests for an accurate determination of the diffusion properties on cementitious materials, J. Electroanal. Chem. 858 (2020) 113791.

[11] C. Andrade, Calculation of chloride diffusion coefficients in concrete from ionic migration measurements, Cem. Concr. Res. 23 (1993) 724-742.

[12] O. Truc, JP. Ollivier, M. Carcassès, A new way for determining the chloride diffusion coefficient in concrete from steady state migration test, Cem. Concr. Res. 30 (2000) 217-226.

[13] H. Friedmann, O. Amiri, A. Aït-Mokhtar, P. Dumargue, A direct method for determining chloride diffusion coefficient by using migration test, Cem. Concr. Res. 34 (2004) 1967-1973.

[14] L. Tang, LO. Nilsson, Rapid determination of the chloride diffusivity in concrete by applying an electrical field, ACI Mater. J. 89 (1992) 49-53.

[15] O. Francy, R. François, Measuring chloride diffusion coefficients from non-steady state diffusion tests, Cem. Concr. Res. 28 (1998) 947-953.

[16] JA. Bogas, A. Gomes, Non-steady-state accelerated chloride penetration resistance of structural lightweight aggregate concrete, Cem. Concr. Compos. 60 (2015) 111-122.

[17] T. Zhang, OE. Gjørv, Effect of ionic interaction in migration testing of chloride diffusivity in concrete, Cem. Concr. Res. 25 (1995) 1535–1542.

[18] H. Friedmann, O. Amiri, A. Aït-Mokhtar, Modelling of EDL effect on chloride migration in cement-based materials, Mag. Concr. Res. 64 (10) (2012) 909–917.

[19] F. He, C. Shi, X. Hu, R. Wang, Z. Shi, Q. Li, P. Li, X. An, Calculation of chloride ion concentration in expressed pore solution of cement-based materials exposed to a chloride salt solution, Cem. Concr. Res. 89 (2016) 168–176.

[20] Y. Yang, RA. Patel, SV. Churakov, NI. Prasianakis, G. Kosakowski, M. Wang, Multiscale modeling of ion diffusion in cement paste: electrical double layer effects, Cem. Concr. Compos. 96 (2019) 55–65.

[21] HE. Álava, E. Tsangouri, N. De Belie, G. De Schutter, Chloride interaction with concretes subjected to a permanent splitting tensile stress level of 65%, Constr. Build. Mater. 127 (2016) 527–538.

[22] D. Li, L. Li, X. Wang, Chloride diffusion model for concrete in marine environment with considering binding effect, Mar. Struct. 66 (2019) 44–51.

[23] S. Chatterji, Mechanism of the CaCl2 attack on Portland cement concrete, Cem. Concr. Res. 8 (1978) 461–467.

[24] FP. Glasser, J. Pedersen, K. Goldthorpe, M. Atkins, Solubility reactions of cement components with NaCl solutions: I. $Ca(OH)_2$ and C-S-H', Adv. Cem. Res. 17 (2005) 57–64.

[25] L. Sutter, K. Peterson, S. Touton, T. Van Dam, D. Johnston, Petrographic evidence of calcium oxychloride formation in mortars exposed to magnesium chloride solution, Cem. Concr. Res. 36 (2006) 1533–1541.

[26] C. Qiao, P. Suraneni, J. Weiss, Damage in cement pastes exposed to NaCl solutions, Constr. Build. Mater. 171 (2018) 120–127.

[27] H.G. Midgley, J.M. Illston, The penetration of chlorides into hardened cement pastes, Cem. Concr. Res. 14 (1984) 546–558.

[28] M. Castellote, C. Andrade, C. Alonso, Changes in concrete pore size distribution due to electrochemical chloride migration trials, ACI Mater. J. 96 (1999) 314–319.

[29] R. Cherif, A. Hamami, A. Aït-Mokhtar, Effects of leaching and chloride migration on the microstructure and pore solution of blended cement pastes during a migration test, Constr. Build. Mater. 240 (2020) 117934.

[30] C. Andrade, M. Castellote, J. Sarria, C. Alonso, Evolution of pore solution chemistry, electro-osmosis and rebar corrosion rate induced by realkalization, Mater. Struct. 32 (1999) 427-436.

[31] M. Castellote, C. Andrade, C. Alonso, Chloride transference numbers in steady-state migration tests, Mag. Concr. Res. 52 (2000) 93–100.

[32] M. Castellote, C. Andrade, C. Alonso, Phenomenological mass-balance-based model of migration tests in stationary conditions: Application to non-steady-state tests, Cem. Concr. Res. 30 (2000) 1885-1893.

[33] M. Castellote, I. Llorente, C. Andrade, C. Alonso, Accelerated leaching of ultra high performance concretes by application of electrical fields to simulate their natural degradation, Mater. Struct. 36 (2003) 81-90.

[34] M. Castellote, X. Turrillas, C. Andrade, C. Alonso, M.A. Rodriguez, Å Kvick, In situ accelerated leaching of cement paste by application of electrical fields monitored by synchrotron X-ray diffraction, Appl. Phys. 79 (2004) 661-669.

[35] LJ. Buckley, MA. Carter, MA. Wilson, JD. Scantlebury, Methods of obtaining pore solution from cement pastes and mortars for chloride analysis, Cem. Concr. Res. 37 (2007) 1544–1550.

[36] A. Kyle, B-P. Bergsma, CM. Hansson, Chloride concentration in the pore solution of Portland cement paste and Portland cement concrete, Cem. Concr. Res. 63 (2014).

[37] VQ. Tran, A. Soive, S. Bonnet, A. Khelidj, A numerical model including thermodynamic equilibrium, kinetic control and surface complexation in order to explain cation type effect on chloride binding capability of concrete, Constr. Build. Mater.191 (2018) 608–618.

[38] VQ. Tran, A. Soive, V. Baroghel-Bouny, Modelisation of chloride reactive transport in concrete including thermodynamic equilibrium, kinetic control and surface complexation, Cem. Concr. Res. 110 (2018) 70–85.

[39] E. Rozière, A. Loukili, F. Cussigh, A performance based approach for durability of concrete exposed to carbonation, Constr. Build. Mater. 23 (2009) 190-199.

[40] E. Rozière, A. Loukili, Performance-based assessment of concrete resistance to leaching, Cem. Concr. Compos. 33 (2011) 451-456.

[41] A. Younsi, P. Turcry, E. Rozière, A. Aït-Mokhtar, A. Loukili, Performance-based design and carbonation of concrete with high fly ash content, Cem. Concr. Compos. 33 (2011) 993–1000.

[42] JA. Bickley, RD. Hooton, KC. Hover, Performance specifications for durable concrete, Concrete Int (2006), 51-57.

[43] NF EN 206-1, Béton – Partie 1: Spécification, performances, production et conformité, avril 2004.

[44] F. Schmidt, FS. Rostasy, A method for calculation of the chemical composition of the concrete pore solution, Cem. Concr. Res. 23 (1993) 1159–1168.

[45] NF P18-459, Concrete – Testing hardened concrete – Testing porosity and density, 2010.

[46] DA. Silva, VM. John, JLD. Ribeiro, HR. Roman, Pore size distribution of hydrated cement pastes modified with polymers, Cem. Concr. Res. 31 (2001) 1177–1184.

[47] A. Aït-Mokhtar, O. Amiri, P. Dumargue, S. Sammartino. A new model to calculate water permeability of cement based materials from MIP results, Adv. Cem. Res. 14 (2002) 43-49.

[48] O. Amiri, A. Aït-Mokhtar, M. Sarhani, Tri-dimensional modelling of cementitious materials permeability from polymodal pore size distribution obtained by mercury intrusion porosimetry tests, Adv. Cem. Res. 17 (2005) 39-45.

[49] L. Zhang, X. Qian, C. Yu, M. Fang, K. Qian, J. Lai, Influence of evaporation rate on pore size distribution, water loss, and early-age drying shrinkage of cement paste after the initial setting, Constr. Build. Mater. 226(2019) 299–306.

[50] A. Aït-Mokhtar, O. Amiri, O. Poupard, P. Dumargue, A new method for determination of chloride flux in cement-based materials from chronoamperometry, Cem. Concr. Compos. 26 (2004) 339–345.

[51] A. Hamami, JM. Loche, A. Aït-Mokhtar, Cement fraction effect on EIS response of chloride migration tests, Adv. Cem. Res. 23 (2011) 233–240.

[52] P. Longuet, L. Burglen, A. Zelwer, The liquid phase of hydrated cement, Rev. Mater. Constr. 676 (1973) 35-41.

[53] RS. Barneyback, S. Diamond, Expression and analysis of pore fluids from hardened cement pastes and mortars, Cem. Concr. Res. 11 (1981) 279–285.

[54] R. Cherif, A. Hamami, A. Aït-Mokhtar, R. Siddique, Comparison of chemical properties of pore solution of hardened cement pastes containing mineral additions, Adv. Cem. Res. 2020, http://doi: 10.1680/jadcr.19.00037.

[55] E. Conforto, N. Joguet, P. Buisson, JE. Vendeville, C. Chaigneau, T. Maugard, An optimized methodology to analyze biopolymer capsules by environmental scanning electron microscopy, Mater. Sci. Eng. C, 47 (2015) 357–366.

[56] C. Rémazeilles, F. Lévêque, E. Conforto, L. Meunier, P. Refait, Contribution of magnetic measurement methods to the analysis of iron sulfides in archaeological waterlogged wood-iron assemblies, Microchem. J. 148 (2019) 10–20.

[57] R. Siddique, Utilization of silica fume in concrete: Review of hardened properties, Resour. Conserv. Recy. 55 (2011) 923-932.

[58] Q. Lü, Q. Qiu, J. Zheng, J. Wang, Q. Zeng, Fractal dimension of concrete incorporating silica fume and its correlations to pore structure, strength and permeability. Constr. Build. Mater. 228 (2019) 116986.

[59] X. Wang, J. Huang, S. Dai, B. Ma, H. Tan, Q. Jiang, Effect of silica fume particle dispersion and distribution on the performance of cementitious materials: A theoretical analysis of optimal sonication treatment time. Constr. Build. Mater. 212 (2019) 549-560.

[60] A. Younsi, P. Turcry, A. Aït-Mokhtar, S. Staquet, Accelerated carbonation of concrete with high content of mineral additions: Effect of interactions between hydration and drying, Cem. Concr. Res. 43 (2013) 25-33.

[61] D. Kong, X. Du, S. Wei, H. Zhang, Y. Yang, SP. Shah, Influence of nano-silica agglomeration on microstructure and properties of the hardened cement-based materials, Constr. Build. Mater. 37 (2012) 707–715.

[62] K. Andersson, B. Allard, M. Bengtsson, B. Magnusson, Chemical composition of cement pore solutions, Cem. Concr. Res. 19 (1989) 327–332.

[63] SA. Greenberg, The chemisorption of calcium hydroxide by silica, J. Phys. Chem. 60 (1956) 325-330, 1956.

[64] S. Urhan, Alkali silica and pozzolanic reactions in concrete. Part 1: Interpretation of published results and a hypothesis concerning the mechanism, Cem. Concr. Res. 17 (1987) 141–152.

[65] C. Lobo, MD. Cohen, Hydration of type K expansive cement paste and the effect of silica fume: II. Pore solution analysis and proposed hydration mechanism, Cem. Concr. Res. 23 (1993) 104–114.

[66] L. Divet, R. Randriambololona, Delayed Ettringite Formation: The Effect of Temperature and Basicity on the Interaction of Sulphate and C-S-H Phase 1, Cem. Concr. Res. 28 (1998) 357–363.

[67] GW. Scherer, Crystallization in pores, Cem. Conc. Res. 29 (1999) 1347–1358.

[68] G. Copin-Montégut, Propriétés physiques de l'eau de mer, Techniques ingénieur, Paris (2002) 79 p.

[69] P. Refait, AM. Grolleau, M. Jeannin, E. François, R. Sabot, Corrosion of mild steel at the seawater/sediments interface: Mechanisms and kinetics, Corros. Sci. 130 (2018) 76–84.

[70] I. Sànchez, XR. Novoa, G. de Vera, MA. Climent, Microstructural modifications in Portland cement concrete due to forced ionic migration tests. Study by impedance spectroscopy, Cem. Concr. Res. 38 (2008) 1015–25.

[71] Q. Huang, C. Wang, Q. Zeng, C. Yang, C. Luo, K. Yang, Deterioration of mortars exposed to sulfate attack under electrical field, Constr. Build. Mater. 117 (2016) 121–128.

Fig. 1. Schematic representation of the two migration test protocols and material sampling for the investigation of the global ionic transport.

Fig. 2. Pore size distributions of the materials before the migration test.

Fig. 3. Chemical composition of CP pore solution before and after the migration test.

Fig. 4. Chemical composition of FA30 pore solution before and after the migration test.

Fig. 5. Chemical composition of PBFS pore solution before and after the migration test.

Fig. 6. Chemical composition of PSF pore solution before and after the migration test.

Fig. 7. Ion concentration gain or loss at the upstream at the end of the migration test.

Fig. 8. Ion concentration gain or loss at the downstream at the end of the migration test.

Fig. 9. SEM images and EDX spectra of CP with and without chloride contamination.

Fig. 10. SEM images and EDX spectra of PFA with and without chloride contamination.

Fig. 11. SEM images and EDX spectra of PBFS with and without chloride contamination.

Fig. 12. Chemical composition of CP* pore solution before and after the migration test.

Fig. 13. Chemical composition of FA30* pore solution before and after the migration test.

Fig. 14. Chemical composition of PBFS* pore solution before and after the migration test.

Fig. 15. Chemical composition of PSF* pore solution before and after the migration test.